SAND2015-2992C

Scaling of Intrusive Stochastic Collocation and Stochastic Galerkin Methods for Uncertainty Quantification in Monte Carlo Particle Transport

Aaron Olson[1], Brian Franke[2], and Anil Prinja[1]

[1]Department of Nuclear Engineering, University of New Mexico, Albuquerque, NM 87131; aolson1@unm.edu; prinja@unm.edu, [2]Sandia National Laboratories, Albuquerque, NM 87185; bcfrank@sandia.gov

Abstract

A Monte Carlo solution method for the system of deterministic equations arising in the application of stochastic collocation (SCM) and stochastic Galerkin (SGM) methods in radiation transport computations with uncertainty is presented for an arbitrary number of materials each containing two uncertain random cross sections. Moments of the resulting random flux are calculated using an intrusive and a non-intrusive Monte Carlo based SCM and two different SGM implementations each with two different truncation methods and compared to the brute force Monte Carlo sampling approach. For the intrusive SCM and SGM, a single set of particle histories is solved and weight adjustments are used to produce flux moments for the stochastic problem. Memory and runtime scaling of each method is compared for increased complexity in stochastic dimensionality and moment truncation. Results are also compared for efficiency in terms of a statistical figure-of-merit.

Stochastic Transport Equation with Generalized Polynomial Chaos

We consider the steady state, single speed transport equation

$$\vec{\Omega}\cdot\nabla\psi(\vec{r},\vec{\Omega},\omega)+\Sigma_t(\vec{r},\omega)\psi(\vec{r},\vec{\Omega},\omega)=\frac{\Sigma_s(\vec{r},\omega)}{4\pi}\phi(\vec{r},\omega) \tag{1}$$

and define total and scattering cross sections as a random perturbation from a distribution, in this case uniform, about the average

$$\Sigma_{t,s}(\vec{r},\omega)=\langle\Sigma_{t,s}(\vec{r})\rangle+\widehat{\Sigma}_{t,s}(\vec{r})\xi_{t,s}(\omega) \tag{2}$$

The 2M-dimensional (M=number of materials) generalized polynomial chaos expansion of the angular flux using random orthogonal polynomials, in this case Legendre polynomials, becomes:

$$\begin{aligned}\psi(\vec{r},\vec{\Omega},\vec{\xi}(\omega))&=\psi(\vec{r},\vec{\Omega},\xi_{t_1}(\omega),\xi_{s_1}(\omega),\cdots\xi_{t_M}(\omega),\xi_{s_M}(\omega))\\&=\sum_{l_1=0}^{\infty}\sum_{m_1=0}^{\infty}\cdots\sum_{l_M=0}^{\infty}\sum_{m_M=0}^{\infty}\psi_{l_1,m_1,\ldots,l_M,m_M}(\vec{r},\vec{\Omega})P_{l_1}(\xi_{t_1}(\omega))P_{m_1}(\xi_{s_1}(\omega))\ldots P_{l_M}(\xi_{t_M}(\omega))P_{m_M}(\xi_{s_M}(\omega))\end{aligned} \tag{3}$$

By the orthogonality of the Legendre polynomials, flux coefficients relate to the angular flux by

$$\begin{aligned}\psi_{l_1,m_1,\ldots,l_M,m_M}(\vec{r},\vec{\Omega})&=a_{l_1m_1\ldots l_Mm_M}\int_{-1}^{1}\int_{-1}^{1}\cdots\int_{-1}^{1}\int_{-1}^{1}\psi(\vec{r},\vec{\Omega},\xi_{t_1},\xi_{s_1},\ldots,\xi_{t_M},\xi_{s_M})\;P_{l_1}(\xi_{t_1})P_{m_1}(\xi_{s_1})\ldots P_{l_M}(\xi_{t_M})P_{m_M}(\xi_{s_M})d\xi_{t_1}d\xi_{s_1}\ldots d\xi_{t_M}d\xi_{s_M}\\a_{l_1m_1\ldots l_Mm_M}&=\prod_{j=1}^{M}(2l_j+1)(2m_j+1)\end{aligned} \tag{4}$$

For notational simplicity define the following:

$$\psi(\vec{r},\vec{\Omega})\equiv\psi_{l_1,m_1,\ldots,l_M,m_M}(\vec{r},\vec{\Omega})\qquad\psi_{m_1-1}(\vec{r},\vec{\Omega})\equiv\psi_{l_1,m_1-1,\ldots,l_M,m_M}(\vec{r},\vec{\Omega}) \tag{5}$$

Eq. (4) is solved two different ways using Monte Carlo particle simulation.

Stochastic Galerkin Method

Using the Legendre polynomial recurrence relationship

$$\xi P_m(\xi)=\frac{m+1}{2m+1}P_{m+1}(\xi)+\frac{m}{2m+1}P_{m-1}(\xi) \tag{6}$$

and projecting the transport equation over the chaos functions produces the following fully coupled system of SGM transport equations

$$\begin{aligned}&\vec{\Omega}\cdot\nabla\psi(\vec{r},\vec{\Omega})+\langle\Sigma_{t,j}\rangle\psi(\vec{r},\vec{\Omega})+\widehat{\Sigma}_{t,j}\left[\left(\frac{l_j+1}{2l_j+3}\right)\psi_{l_j+1}(\vec{r},\vec{\Omega})+\left(\frac{l_j}{2l_j-1}\right)\psi_{l_j-1}(\vec{r},\vec{\Omega})\right]=\\&\qquad\frac{\langle\Sigma_{s,j}\rangle}{4\pi}\phi(\vec{r})+\frac{\widehat{\Sigma}_{s,j}}{4\pi}\left[\left(\frac{m_j+1}{2m_j+3}\right)\phi_{m_j+1}(\vec{r})+\left(\frac{m_j}{2m_j-1}\right)\phi_{m_j-1}(\vec{r})\right],\;l_1,m_1,\ldots,l_M,m_M=0,\infty\end{aligned} \tag{7}$$

Stochastic Collocation Method

Instead approximating Eq. (4) with a multidimensional quadrature rule of order K where ξ values are taken at quadrature nodes gives

$$\begin{aligned}\psi_{l_1,m_1,\ldots,l_M,m_M}(\vec{r},\vec{\Omega})\approx a_{l_1m_1\ldots l_Mm_M}\sum_{k_1=1}^{K}\sum_{n_1=1}^{K}\cdots\sum_{k_M=1}^{K}\sum_{n_M=1}^{K}&w_{k_1}w_{n_1}\ldots w_{k_M}w_{n_M}\\&\psi_{k_1n_1\ldots k_Mn_M}(\vec{r},\vec{\Omega})P_{l_1}(\xi_{t_1}^{k_1})P_{m_1}(\xi_{s_1}^{n_1})\ldots P_{l_M}(\xi_{t_M}^{k_M})P_{m_M}(\xi_{s_M}^{n_M})\end{aligned} \tag{8}$$

such that the flux coefficients are acquired by solving a system of uncoupled equations equal to instances of Eq. (1) at collocation points:

$$\vec{\Omega}\cdot\nabla\psi(\vec{r},\vec{\Omega},\omega)+\Sigma_t(\vec{r},\omega)\psi(\vec{r},\vec{\Omega},\omega)=\frac{\Sigma_s(\vec{r},\omega)}{4\pi}\phi(\vec{r},\omega) \tag{9}$$

Truncation Methods

The "total-order" truncation, labeled SG-1, by setting flux coefficients to 0 for

$$\sum_{k=1}^{M}l_k+m_k\geq K \tag{10}$$

The "tensor-product" truncation, labeled SG-2, sets the flux coefficients to 0 for

$$l_k\geq K\qquad m_k\geq K \tag{11}$$

SGM Solution Methods

The SGM implementations solve the fully coupled set of equations (Eq. (7)) applying the SG-1 or SG-2 truncation as a closure, written here in vector form as

$$\vec{\Omega}\cdot\nabla\mathbf{\Psi}+\mathbf{A_t}\mathbf{\Psi}=\widehat{\mathbf{A}}_\mathbf{t}\mathbf{\Psi}+\frac{\widehat{\mathbf{A}}_\mathbf{s}}{4\pi}\mathbf{\Phi} \tag{12}$$

utilizing the following matrix definitions:

$$\mathbf{A_t}=\begin{pmatrix}\langle\widehat{\Sigma}_t\rangle&0&0&0&\ldots&0&0\\0&\langle\widehat{\Sigma}_t\rangle&0&0&\ldots&0&0\\0&0&\langle\widehat{\Sigma}_t\rangle&0&\ldots&0&0\\0&0&0&\langle\widehat{\Sigma}_t\rangle&\ddots&0&0\\\vdots&\vdots&\vdots&\ddots&\ddots&\ddots&\vdots\\0&0&0&0&\ddots&\langle\widehat{\Sigma}_t\rangle&0\\0&0&0&0&\ldots&0&\langle\widehat{\Sigma}_t\rangle\end{pmatrix}\widehat{\mathbf{A}}_\mathbf{t}=\begin{pmatrix}0&\frac{1}{3}\widehat{\Sigma}_t&0&0&\ldots&0&0\\\widehat{\Sigma}_t&0&\frac{2}{5}\widehat{\Sigma}_t&0&\ldots&0&0\\0&\frac{2}{3}\widehat{\Sigma}_t&0&\frac{3}{7}\widehat{\Sigma}_t&\ldots&0&0\\0&0&\frac{3}{5}\widehat{\Sigma}_t&0&\ddots&0&0\\\vdots&\vdots&\vdots&\ddots&\ddots&\ddots&\vdots\\0&0&0&0&\ddots&0&\frac{K-1}{2K-1}\widehat{\Sigma}_t\\0&0&0&0&\ldots&\frac{K-1}{2K-3}\widehat{\Sigma}_t&0\end{pmatrix}\widehat{\mathbf{A}}_\mathbf{s}=\begin{pmatrix}\langle\Sigma_s\rangle&\frac{1}{3}\widehat{\Sigma}_s&0&0&\ldots&0&0\\\widehat{\Sigma}_s&\langle\Sigma_s\rangle&\frac{2}{5}\widehat{\Sigma}_s&0&\ldots&0&0\\0&\frac{2}{3}\widehat{\Sigma}_s&\langle\Sigma_s\rangle&\frac{3}{7}\widehat{\Sigma}_s&\ldots&0&0\\0&0&\frac{3}{5}\widehat{\Sigma}_s&\langle\Sigma_s\rangle&\ddots&0&0\\\vdots&\vdots&\vdots&\ddots&\ddots&\ddots&\vdots\\0&0&0&0&\ddots&\langle\Sigma_s\rangle&\frac{K-1}{2K-1}\widehat{\Sigma}_s\\0&0&0&0&\ldots&\frac{K-1}{2K-3}\widehat{\Sigma}_s&\langle\Sigma_s\rangle\end{pmatrix} \tag{13}$$

Both implementations account for the first two terms in Eq. (12) by sampling distance to collision or interface.

The first implementation, designated SG-I, couples moments through particle interactions. Once the location of a collision has been determined, Eq. (14) is sampled against to decide if the collision is a particle scatter or streaming event.

$$f_s=\frac{\langle\Sigma_s\rangle+\widehat{\Sigma}_s}{\widehat{\Sigma}_t+\langle\Sigma_s\rangle+\widehat{\Sigma}_s} \tag{14}$$

For either outcome, a weight matrix of flux coefficients is modified according to the corresponding operation from Eq. (15) such that the chosen event outcome is in effect solved in each coupled equation.

$$\mathbf{w_o}=-\mathbf{w_i}\frac{1}{1-f_s}\frac{\widehat{\mathbf{A}}_\mathbf{t}}{\langle\Sigma_t\rangle}\qquad\qquad\mathbf{w_o}=\mathbf{w_i}\frac{1}{f_s}\frac{\widehat{\mathbf{A}}_\mathbf{s}}{\langle\Sigma_t\rangle} \tag{15}$$

The second implementation, designated SG-S, increases coupling of moments during simulation by adjusting the weight matrix at every sampled distance and particle scatter separately. Again according to Eq. (12), weight adjustments due to a collision or streaming event are performed using the first and third terms of Eq. (12) as the set of eigenvalue problems

$$\widehat{\mathbf{A}}_\mathbf{t}\vec{\psi}=\lambda\vec{\psi} \tag{16}$$

where $\vec{\psi}$ is a vector in the total cross section dimension. The general solution along with coefficient normalization are found in Eq. (17).

$$\vec{\psi}(\vec{r}_0+s\vec{\Omega})=\sum_{j=1}^{J}c_j\vec{V}_j\exp(\lambda_js)\qquad\qquad\sum_{j=1}^{J}c_j\vec{V}_j=\vec{\psi}(\vec{r}_0) \tag{17}$$

Note that the normalization must be calculated for each vector size J, such that the SG-1 truncation requires K-1 normalization solves for each event and material. The first and last terms of Eq. (12) are written as

$$\vec{\Omega}\cdot\nabla\mathbf{\Psi}=\frac{\langle\Sigma_s\rangle}{\langle\Sigma_t\rangle}\frac{\widehat{\mathbf{A}}_\mathbf{s}}{\langle\Sigma_s\rangle}\int_{4\pi}\mathbf{\Psi}d\Omega \tag{18}$$

and moderate weight adjustment for interactions. The integral is evaluated by randomly sampling a new direction, the first fraction is incorporated in survival biasing, and the second requires a matrix operation.

SCM Solution Methods

The Correlated Random Number Stochastic Collocation implementation (CR-SC) solves all histories at each collocation point, but begins the histories at each point with the same random number seed.

The Correlated Sampling Stochastic Collocation implementation (CS-SC) only solves particle histories for a baseline point, then calculates event outcomes at collocation points with weight adjustment ratios based on correlated sampling of the general form:

$$w_{o,k_1,n_1,\ldots,k_M,n_M}=\frac{p_{k_1,n_1,\ldots,k_M,n_M}}{p_{sim}}w_{i,k_1,n_1,\ldots,k_M,n_M} \tag{19}$$

For distance to collision operations and scattering operations this form becomes those in Eq. (20) respectively.

$$w_{o,k_1,n_1,\ldots,k_M,n_M}=\frac{\langle\Sigma_t\rangle+\widehat{\Sigma}_t\xi_t^{k_i}}{\langle\Sigma_t\rangle}\exp\left[-\widehat{\Sigma}_t\xi_t^{k_i}s\right]w_{i,k_1,n_1,\ldots,k_M,n_M}\qquad w_{o,k_1,n_1,\ldots,k_M,n_M}=\frac{\langle\Sigma_s\rangle+\widehat{\Sigma}_s\xi_s^{k_i}}{\langle\Sigma_t\rangle+\widehat{\Sigma}_t\xi_t^{k_i}}w_{i,k_1,n_1,\ldots,k_M,n_M} \tag{20}$$

Memory Scaling

The simplex-shaped weight array of the SG-1 truncation method scales as the binomial coefficients:

$$\binom{2M+K}{K} \tag{21}$$

The hyper-cube-shaped weight array of the SG-2 truncation method scales as the exponential:

$$K^{2M} \tag{22}$$

Table 1: SG-1 Weight Matrix Size

	K=2	K=3	K=4	K=5	K=6
M=1	3	6	10	15	21
M=2	5	15	35	70	126
M=3	7	28	84	210	462
M=4	9	45	165	495	1287
M=5	11	66	286	1001	3003
M=6	13	91	455	1820	6188

Table 2: SG-2 Weight Matrix Size

	K=2	K=3	K=4	K=5	K=6
M=1	4	9	16	25	36
M=2	16	81	256	625	1296
M=3	64	729	4096	1.6E4	4.7E4
M=4	256	6561	6.6E4	3.9E5	1.7E6
M=5	1024	5.9E4	1.0E6	9.8E6	6.0E7
M=6	4096	5.3E5	1.7E7	2.4E8	2.2E9

Runtime Scaling

The runtime per history solved is compared to the average runtime for a benchmark history:
(runtime/(#histories * #points))/(average runtime).
This metric does not consider accuracy of results, but provides scaling efficiency of computational solve against a benchmark solution.

Table 3: Runtime Scaling Material Arrangements

# mats	cell 1	cell 2	cell 3	cell 4	cell 5	cell 6	cell 7	cell 8	cell 9	cell 10
1	1	1	1	1	1	1	1	1	1	1
2	1	2	1	2	1	2	1	2	1	2
3	1	2	3	1	2	3	1	2	3	1
4	1	2	3	4	1	2	3	4	1	2
5	1	2	3	4	5	1	2	3	4	5

Figures 1-6: Runtime Scaling

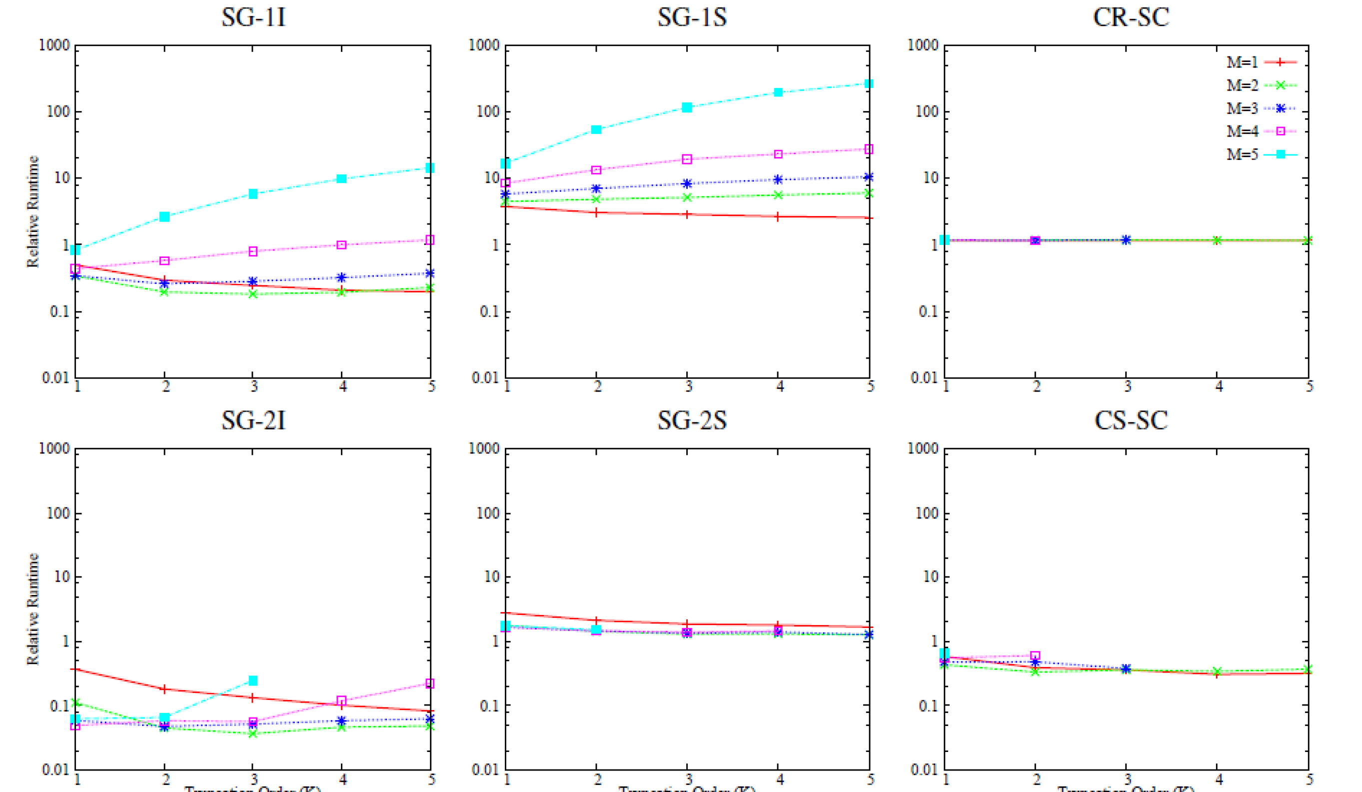

Transmission Results

Table 4 defines a two material and three material test problem used for transmission and Figure-of-Merit results, where materials 1 and 3 have the same physical properties.

Table 4: Material Definitions and Arrangements

Mat #/(cm^{-1})	$\langle\Sigma_t\rangle$	$\langle\Sigma_s\rangle$	$\widehat{\Sigma}_t$	$\widehat{\Sigma}_s$
2	5.0	3.5	1.0	0.4
1 or 3	5.0	1.0	0.5	0.4
Mat Arrng.:	*1*	*2*	*2*	*1 or 3*

Figures 7-8: Transmission PDFs SG-1S(top) SG-2S(bot)

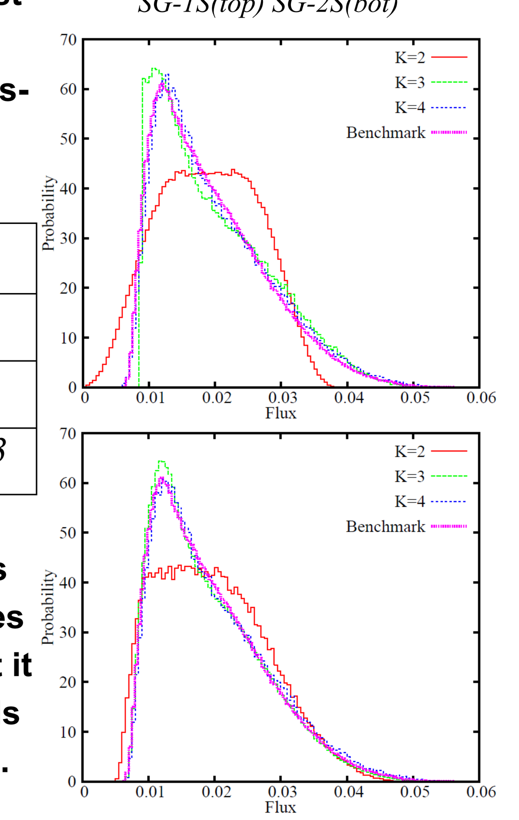

Figures 7 and 8 show PDFs of transmission results for SG-1S and SG-2S with various truncation orders K. For the same truncation order K, SG-2S produces better results, especially further from the mean, but it also requires solving more moments. Both methods appear to be converging to the benchmark solution.

Figure of Merit Results

A Figure of Merit (FOM) is defined which compares relative error (R) and computational time (T) such that the higher the FOM value, the quicker the convergence of the moment:

$$FOM=\frac{1}{R^2T}$$

This FOM is solved for three combinations of K and M physically defined in Table 4.

Figures 4-6: FOM values for M=2, K=3(top); M=2, K=4(middle); and M=3, K=4(bottom)

Flux Moment		Figure of Merit						
			SCM		SGM			
l_1,m_1,l_2,m_2	ψ_{l_1,m_1,l_2,m_2}	MC	CR-SC	CS-SC	SG-1I	SG-2I	SG-1S	SG-2S
0,0,0,0	1.9E-2	1.9E+0	8.4E+1	1.7E+2	6.8E+2	4.9E+2	2.4E+2	1.4E+2
1,0,0,0	-1.2E-2	3.6E-2	2.5E+1	1.3E+2	2.4E+2	1.8E+2	1.5E+2	9.0E+1
2,0,0,0	3.0E-3	1.2E-3	1.3E+0	6.4E+1	2.4E+1	1.7E+1	5.8E+1	3.4E+1
1,1,0,0	-2.7E-3	4.9E-4	1.7E+1	7.7E+1	2.7E+1	1.8E+1	2.4E+1	1.3E+1
2,2,0,0	1.3E-4	*a*	2.5E+0	2.5E+1	*b*	5.3E-1	*b*	1.7E+0
1,1,1,1	1.0E-4	*a*	1.3E+1	7.0E+1	*b*	*a*	*b*	9.6E-1
2,2,2,2	1.3E-7	*a*	2.4E-1	4.2E+1	*b*	*a*	*b*	2.1E-2
Time (s):		2.9E+6	21437	7759	600	843	3649	5941

Flux Moment		Figure of Merit						
			SCM		SGM			
l_1,m_1,l_2,m_2	ψ_{l_1,m_1,l_2,m_2}	MC	CR-SC	CS-SC	SG-1I	SG-2I	SG-1S	SG-2S
0,0,0,0	1.9E-2	1.9E+0	3.4E+1	5.2E+1	2.7E+2	1.6E+2	9.1E+1	5.0E+1
1,0,0,0	-1.2E-2	3.6E-2	1.3E+1	3.9E+1	9.6E+1	5.9E+1	5.6E+1	3.1E+1
2,0,0,0	3.0E-3	1.2E-3	6.3E-1	1.9E+1	8.9E+0	5.3E+0	2.0E+1	1.1E+1
3,0,0,0	-5.4E-4	3.1E-5	1.7E-2	7.1E+0	1.5E+0	9.1E-1	5.9E+0	3.1E+0
1,1,0,0	-2.7E-3	4.9E-4	8.3E+0	2.4E+1	1.0E+1	6.2E+0	9.9E+0	4.6E+0
2,2,0,0	1.4E-4	*a*	9.1E-1	7.1E+0	*b*	1.5E-1	*b*	5.2E-1
3,3,0,0	-5.7E-6	*a*	1.1E-1	2.2E+0	*b*	4.6E-2	*b*	7.6E-2
1,1,1,1	1.1E-4	*a*	4.8E+0	2.1E+1	*b*	*a*	*b*	3.3E-1
2,2,2,2	1.4E-7	*a*	1.3E-1	1.0E+1	*b*	*a*	*b*	*a*
3,3,3,3	1.3E-10	*a*	1.2E-3	3.3E+1	*b*	*a*	*b*	*a*
Time (s):		2.9E+6	66363	25318	1526	2558	8994	17295

Flux Moment		Figure of Merit						
			SCM		SGM			
l_1,m_1,l_2,m_2	ψ_{l_1,m_1,l_2,m_2}	MC	CR-SC	CS-SC	SG-1I	SG-2I	SG-1S	SG-2S
0,0,0,0,0,0	1.9E-2	3.9E+0	1.3E+0	1.6E+0	4.9E+1	6.7E+0	1.2E+1	1.6E+0
1,0,0,0,0,0	-5.1E-3	1.8E-3	1.3E+0	2.1E+0	8.3E+0	1.1E+0	1.2E+1	1.5E+0
2,0,0,0,0,0	5.4E-4	*a*	1.1E-2	2.6E+0	5.0E-1	6.9E-2	5.4E+0	6.9E-1
3,0,0,0,0,0	-4.9E-5	*a*	1.6E-4	7.4E-1	1.2E-1	1.2E-2	6.5E-1	6.7E-2
1,1,0,0,0,0	-3.7E-4	1.9E-4	2.2E-1	1.4E+0	5.1E-1	7.2E-2	5.4E-1	6.9E-2
2,2,0,0,0,0	1.3E-5	*a*	4.5E-2	2.9E-1	*b*	*a*	*b*	3.4E-3
3,3,0,0,0,0	-4.2E-7	*a*	3.0E-3	3.8E-2	*b*	*a*	*b*	*a*
1,1,1,1,1,1	-1.9E-6	*a*	4.8E-2	3.7E-1	*b*	*a*	*b*	3.3E-3
2,2,2,2,2,2	8.8E-11	*a*	1.4E-4	2.0E-2	*b*	*a*	*b*	*a*
3,3,3,3,3,3	*a*	*a*	*a*	*a*	*b*	*a*	*b*	*a*
Time (s):		2.4E+7	1.1E+6	5.5E+5	6835	49801	34087	2.6E+5

a FOM values omitted due to poor statistical convergence
b Moment not calculated with this truncation method

Conclusions

- **All SCM and SGM methods outperformed brute force Monte Carlo in FOM**
- **SCM implementations converged the most moments**
- **SGM implementations produced best FOM values for lower-order moments**

- **CS-SC solved more moments more efficiently than other methods, but is intrusive**
- **CR-SC produced much better results than brute-force Monte Carlo and is non-intrusive**
- **SCM implementations may be improved upon using sparse or anisotropic grids**

- **SG-1 truncation requires less memory and solves more quickly than SG-2**
- **SG-2 more accurate than SG-1 for same truncation order**
- **SG-1 may be only choice as complexity increases**
- **SG-I implementation produced better FOM values for lower moments than SG-S**
- **SG-S resolved more higher moments than SG-I**

Acknowledgements

The first author gratefully acknowledges the support of the Department of Energy under the Nuclear Energy University Programs Graduate Fellowship. Sandia National Laboratories is a multi-program laboratory managed and operated by Sandia Corporation, a wholly owned subsidiary of Lockheed Martin Corporation, for the U.S. Department of Energy's National Nuclear Security Administration under contract DE-AC04-94AL85000. A special thanks also to Bob Clancy at SNL for printing this poster.

References

[1] R. G. Ghanem and P. D. Spanos, *Stochastic finite elements: a spectral approach*, Dover (2003).
[2] L. Mathelin, M. Y. Hussaini, and T. A. Zang, "Stochastic Approaches to Uncertainty Quantification in CFD simulations," *Numer. Algorithms*, 38, pp. 209 (2005).
[3] M. M. R. Williams, "Polynomial Chaos Functions and Neutron Diffusion," *Nucl. Sci. Eng.*, 155, pp. 109 (2007).
[4] E. D. Fichtl and A. Prinja, "The Stochastic Collocation Method for Radiation Transport in Random Media," *Journal of Quantitative Spectroscopy and Radiative Transfer*, 112, pp. 646 (2011).
[5] E. D. Fichtl, *Stochastic Methods for Uncertainty Quantification in Radiation Transport*, The University of New Mexico (2009).
[6] B. C. Franke and A. K. Prinja, "Efficient Monte Carlo Solution for Uncertainty Propagation with Stochastic Collocation," *Tran. Am. Nucl. Soc.*, 106, pp. 346 (2012).
[7] B. C. Franke and A. K. Prinja, "Monte Carlo Solution for Uncertainty Propagation in Particle Transport with a Stochastic Galerkin Method," *International Conference on Mathematics and Computational Methods Applied to Nuclear Science & Engineering (M&C 2013)*, Sun Valley, ID, May, 2013, American Nuclear Society.